Bioorganic & Medicinal Chemistry 28 (2020) 115596

Contents lists available at ScienceDirect

Bioorganic & Medicinal Chemistry

journal homepage: www.elsevier.com/locate/bmc

Amide derivatives of Gallic acid: Design, synthesis and evaluation of inhibitory activities against *in vitro* α-synuclein aggregation

Li Chen[a,d], Guo-Long Huang[a,d], Ming-Huan Lü[a], Yun-Xiao Zhang[a,*], Ji Xu[b,*], Su-Ping Bai[c,*]

[a] College of Chemistry and Institute of Green Catalysis, Zhengzhou University, Daxue Road 75, 450052 Zhengzhou, China
[b] School of Basic Medical Science, Neuroscience Research Institute, Academy of Medical Sciences, Zhengzhou University, Kexue Road 100, 450001 Zhengzhou, China
[c] College of Pharmacy, Xinxiang Medical University, Jinsui Road 601, 453003 Xinxiang, China

ARTICLE INFO

Keywords:
Amide derivatives of Gallic acid
Synthesis
α-Synuclein
Anti-aggregation
Inhibitor

ABSTRACT

Gallic acid (GA), a natural phenolic acid, has received numerous attention because of its anti-oxidative, anti-inflammatory, and anti-cancer activity. More importantly, GA can act as an efficient inhibitor of α-Synuclein (α-Syn) aggregation at early stages. Nevertheless, some evidences suggest that GA is unlikely to cross the blood–brain barrier because of its high hydrophilicity. Hence, GA may not be considered as a promising candidate or entering brain and directly affecting the central nervous system. Accordingly, we have designed and synthesized a series of amide derivatives of GA, some of which possess appropriate lipophilicity and hydrophilicity with LogP (2.09–2.79). Meanwhile, these sheet-like conjugated compounds have good π-electron delocalization and high ability of hydrogen-bond formation. Some compounds have shown better *in vitro* anti-aggregation activities than GA towards α-Syn, with IC_{50} down to 0.98 μM. The valid modification strategy of GA is considered an efficient way to discover novel inhibitors of α-Syn aggregation.

1. Introduction

Parkinson's disease (PD) is one of the most common neurodegenerative diseases. It is characterized primarily by the loss of dopaminergic neurons in the substantia nigra, which led to movement disorders.[1] Although the precise molecular pathogenesis of PD are unknown, the misfolding and aggregation of the abundant neuronal protein α-synuclein (α-Syn) are involved in all PD cases.[2] A large number of conclusive evidence had been found that α-Syn oligomers, protofibrils and amyloid fibrils are neurotoxic, and have shown prion-like pathology propagation.[3,1b] Hence, maintaining α-Syn proteostasis is considered as a key approach to PD prophylaxis and treatment.

Up to date, a number of natural and synthesized small molecular compounds have been reported as the optional inhibitor of α-Syn aggregation.[4] Particularly, polyphenols showed good inhibitory activities.[5] There are two sub-categories of polyphenol, flavonoids and phenolic acids. Examples of flavonoids include flavonols, flavones, isoflavones, flavanones, anthocyanidins, and flavanols.[6] On the other hand, phenolic acids include protocatechuic acid, gallic acid, caffeic acid, ferulic acid, rosmarinic acid, chlorogenic acid, etc [7] (Scheme 1). Polyphenols may exhibit their neuroprotection through a variety of molecular mechanisms, such as the anti-oxidantion, anti-apoptosis, anti-inflammation and anti-aggregation effects on α-Syn, amyloid-beta (Aβ) and tau proteins.[5b,6]

GA (Scheme 1), a natural phenolic acid, has been found abundant in grapes, berries, wine and tea. In recent years, GA received significant attention because of its potent anti-oxidative activity to scavenge reactive oxygen species and prevent lipid peroxidation.[8] GA also possesses anti-inflammatory and anti-cancer activity.[9] More importantly, various studies have demonstrated that GA prevents proteins from misfolding as well as reduces the cell toxicity induced by fibrillar protein aggregates.[10] Specifically, GA interacts with α-Syn to prevent structural transition to a more compact form that precedes fibril formation. As a result, GA acts as an efficient inhibitor of α-Syn aggregation at the early stages.[7c,10b,11]

Nevertheless, some evidence suggest that phenolic acids, such as ferulic acid and chlorogenic acid, are unlikely to cross the blood–brain barrier (BBB).[12a] Hence, GA may face the same challenge as a promising candidate for entering brain and for a direct effect on the central nervous system (CNS). In addition, the desired range of lipophilicity (LogP value) for candidate molecule crossing BBB is usually from 1 to 5,[4] and there is statistics-based analytical results showed that a LogP < 1.5 is detrimental for reaching the CNS.[12b] The LogP value of GA is about 0.42, which is a rather hydrophilic molecule. Accordingly, the valid

* Corresponding authors.
E-mail addresses: zhangyx@zzu.edu.cn (Y.-X. Zhang), xuji@zzu.edu.cn (J. Xu), baisuping@xxmu.edu.cn (S.-P. Bai).
[d] These authors contributed equally.

https://doi.org/10.1016/j.bmc.2020.115596
Received 3 April 2020; Received in revised form 31 May 2020; Accepted 9 June 2020
Available online 17 June 2020

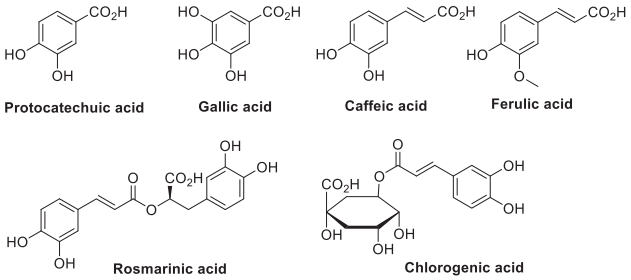

Scheme 1. Reported natural phenolic acid inhibitors on α-Syn aggregation.

modification of GA which enhance its lipophilicity and anti-aggregation performance on α-Syn, should be an efficient approach to discover novel inhibitors of α-Syn aggregation.

Based on the present evidence above and our hypothesis,[4] we focus on design suitable small molecules containing phenolic acids, which have strong binding force with the core of non-amyloid-beta component (NACore), interfere with the formation of β-sheets structure, block the formation of oligomer nuclei in early stage, and further prevent the development of α-Syn fibrillation. In the present work, a series of amide derivatives of GA and other phenolic acids were design and synthesized, which possess sheet-like conjugated structure and suitable LogP value. Their inhibitory activities against α-Syn aggregation were evaluate and the structure–activity-relationship (SAR) studies were studied.

2. Results and discussion

2.1. Chemistry

Based on our previous work,[4] we designed a series of aromatic amide derivatives, which possess sheet-like conjugated structure as the potential inhibitor of α-Syn aggregation. The first series of compounds was unilateral or bilateral flurobenzoyl *p*- phenylenediamines (**1a-1f** and **1aa-1fe**). As our main goal, the second series of compounds containing phenolic acyl were designed as *N*-acyl *p*-phenylenediamines and *N,N′*-diacyl *p*-phenylenediamines (**1g-1gi** and **2aa-2ba**). Furthermore, as the most impotant analogues with exposed hydroxyl, **3g**, **3gd-3gi** and **4aa-4ba** were prepared *via* demethylation reaction.

Firstly, the *N*-acyl *p*-phenylenediamine compounds as intermediates (**1a-1g** and **2a-2b**) were prepared from *p*-phenylenediamine and different carboxylic acids, such as fluorobenzoic acids, 3,4,5-trimethoxybenzoic acid, sulfonic acids and (*E*)-3-(pyridin-4-yl)acrylic acid *via* mono-acylation in medium yields. These reactions were carry out using 2-(7-azobenzotriazole)-*N, N, N′, N′*-tetramethylurea hexafluorophosphate (HATU) as coupling agent and triethylamine as base.[13] Furthermore, *N,N′*-diacyl *p*-phenylenediamines were synthesized by the similar approaches. Compound **1aa-1gi** and **2aa-2bb** were obtained from **1a to 1g** and **2a-2b** *via* further acylation under HATU/ triethylamine in medium to high yields (Scheme 2).

The amide derivatives of GA with "exposed hydroxyl"(**3g**, **3gd-3gi** and **4aa-4ba**) were obtained by demethylation of **1g**, **1gd-1gi** and **2aa-2ba** respectively under boron tribromide in medium to high yields (Scheme 3).[14]

2.2. Biological evaluation

2.2.1. In vitro inhibitory activities of the synthesized compounds against α-Syn aggregation by ThT fluorescence assay

Thioflavin T (ThT) fluorescence assay is a valid method to evaluate the inhibitory activities of compounds against α-Syn aggregation. ThT shows weak fluorescence intensity (FI) in monomeric α-Syn, α-Syn oligomer nuclei or in α-Syn fibril-free system. On the contrary, ThT displays strong FI in the presence of α-Syn fibrils. ThT FI can quantitatively reflect the kinetics and abilities of compounds inhibiting towards α-Syn aggregation. Based on our previous work,[4] The ThT fluorescence maximum emission wavelength were optimized as 482 nm (λ_{em} = 482 nm) under excitation light at 450 nm (λ_{ex} = 450 nm). The method of inhibitory activities investigation of compounds was described in supporting materials. The ThT FI of blank group was measured without compound, and thereby obtained the maximal FI. The FI value of blank group was set as 1 (100%). The ratio of FI of the tested system within compound to that of blank group was defined as the relative fluorescence intensity (RFI) (Fig. 1). In fact, there was a positive correlation between the percent reduction of RFI and the inhibitory activity of the evaluated compound.

In detail, the RFIs of first series of compounds—fluorobenzoyl *p*-phenylenediamines (**1aa-1fe**) were shown in Fig. 1A. The RFIs of second series of compounds, diacyl *p*-phenylenediamines containing methyl-protected-GA (**1ga-1gi and 2aa-2ba**, except **2bb**) were shown in Fig. 1B. More importantly, Fig. 1C showed the RFIs of mono- or diacyl *p*-phenylenediamines containing GA (**3g**, **3gd-3gi** and **4aa-4ba**), GA and other mono-acyl *p*-phenylenediamines without GA component as control (**1b-1f** and **2a-2b**). In order to describe the inhibition activity more conveniently, the ThT RFI was transformed to α-Syn aggregation inhibition ratio by the formula: α-Syn aggregation inhibition ratio = 100% (RFI of blank group)-x% (RFI of compound group). In summary, the lower RFI corresponding to the higher inhibitory activity against α-Syn aggregation, thereby the ratio intuitively reflected the inhibitory activity of compound (Tables 1–3).

From Table 1, this series of compounds have shown the inhibitory ratio towards α-Syn aggregation from 1.9% to 42.1%. Compounds **1ab-1ae** were comprised of benzoyl and fluorobenzoyl moieties liked by *p*-phenylenediamine, and only **1ae** containing block of tetrafluorobenzoyl displayed more than 30% inhibition ratio (31.2%). Compounds **1fb-1fe** were comprised of (*E*)-3-(pyridin-4-yl)acryloyl and fluorobenzoyl moieties, among of which, **1fc** and **1fd** displayed 42.1% and 31.4% inhibition ratio, respectively. Apparently, **1fc** containing 2,4-difluorobenzoyl has shown better inhibitory activity than **1fd**. Other compounds containing bi-fluorobenzoyl blocks have shown lower inhibitory activities.

From Table 2, compounds **1ga-1gi** contain block of methyl-protested gallic acyl on one side, and on the other side, the blocks are substituted benzoyls groups or (*E*)-3-(pyridin-4-yl)acryloyl. Compound **1gd** with (*E*)-3-(pyridin-4-yl)acryloyl demonstrated slight higher ratio (33.5%) than **1ga**, **1gb**, **1gc** and **1gf**, which contain benzoyl or fluorobenzoyl on the same side (17.7%, 11.8%, 10.4% and 4.9%). Fortunately, compound **1gi**, *N,N'*-di(3,4,5-trimethoxybenzoyl) *p*-phenylenediamine, has shown good inhibitory activity (83.4%).

Compounds **2aa-2ba** contain block of methyl-protested gallic acyl on one side, and on the other side, sulfonyls. Tosylate analogue **2aa** showed better ratio than **2ba**, which possessed pyridine-3-sulfonyl group (34.1% vs 22.7%). In particular, compound **2bb**, *N,N'*-di(pyridine-3-sulfonyl) *p*-phenylenediamine, has shown medium inhibitory activity (57.2%).

Table 3 indicated various inhibitory activities with different amide derivatives of GA. Firstly, mono-amide derivatives of *p*-phenylenediamine, **1f**, **1b** and **1c** displayed the decreasing trend of inhibitory activities (42.4%, 34.1% and 16.6%). Mono-sulfonamide derivatives **2a** and **2b**, also showed low ratio (15.9% and 15.4%). Noticeably, they all have lower inhibitory activities than that of GA (78.2%). On the contrary, **3g** (*N*-gallic acyl *p*-phenylenediamine) demonstrated a higher activity (84.2%) than GA.

For the bi-amide derivatives, **3gd-3gi** and **4aa-4ba** have shown medium to high inhibitory activities from 39.0% to 94.4%. Compounds **3gd-3gi** contained one block of gallic acyl and another block of substituted benzoyl. Among these analogues, **3gf** containing fluorobenzoyl groups displayed outstanding activity comparing with its corresponding precursor **1gf** (Table 2) (85.8% vs 4.9%). The similar trend was found in **3gd** and **1gd** (48.9% vs 33.5%). Surprisingly, **3gi** which containing two identical gallic acyl groups displayed lower ratio comparing with

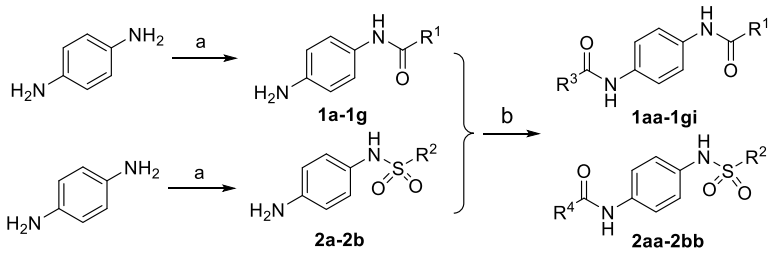

1a:R^1=phenyl;
1aa:R^3=phenyl; **1ab**:R^3=4-fluorophenyl;
1ac:R^3=2,4-difluorophenyl;
1ad:R^3=3,4-difluorophenyl;
1ae:R^3=2,3,4,5-tetrafluorophenyl
1b:R^1=4-fluorophenyl;
1ba:R^3=4-fluorophenyl;
1bb:R^3=2,4-difluorophenyl;
1bc:R^3=3,4-difluorophenyl;
1bd:R^3=2,3,4,5-tetrafluorophenyl
1c:R^1=2,4-difluorophenyl;
1ca:R^3=2,4-difluorophenyl;
1cb:R^3=3,4-difluorophenyl;
1cc:R^3=2,3,4,5-tetrafluorophenyl
1d:R^1=3,4-difluorophenyl;
1da:R^3=3,4-difluorophenyl;
1db:R^3=2,3,4,5-tetrafluorophenyl
1e:R^1=2,3,4,5-tetrafluorophenyl;
1ea:R^3=2,3,4,5-tetrafluorophenyl
1f:R^1=(*E*)-2-(pyridin-4-yl)vinyl
1fa:R^3=phenyl;
1fb:R^3=4-fluorophenyl;
1fc:R^3=2,4-difluorophenyl;
1fd:R^3=3,4-difluorophenyl;
1fe:R^3=2,3,4,5-tetrafluorophenyl
1g:R^1=3,4,5-trimethoxyphenyl;
1ga:R^3=phenyl;
1gb:R^3=3,4-difluorophenyl;
1gc:R^3=2,3,4,5-tetrafluorophenyl;
1gd:R^3=(*E*)-2-(pyridin-4-yl)vinyl;
1ge:R^3=4-fluorophenyl;
1gf:R^3=2,4-difluorophenyl;
1gg:R^3=2-methylphenyl;
1gh:R^3=4-methxoyphenyl;
1gi:R^3=3,4,5-trimethoxyphenyl
2a:R^2=4-methylphenyl;
2aa:R^4=3,4,5-trimethoxyphenyl
2b:R^2=3-pyridinyl;
2ba:R^4=3,4,5-trimethoxyphenyl;
2bb:R^4=3-pyridinyl

Scheme 2. Preparation of *N*-acyl *p*-phenylenediamines and *N,N′*-diacyl *p*-phenylenediamines. Reagents and conditions: a) CH_2Cl_2, HATU, trimethylamine, R^1COOH or R^2SO_3H, rt, 5 h, 45–55%; b) CH_2Cl_2, HATU, trimethylamine, R^3COOH or R^4COOH, rt, 5 h, 60–77%.

1gi (39.0% vs 83.4%). Compounds **4aa-4ba** possess similar structure with **3gd-3gi**, with sulfonyl groups serves the other acyl block. Comparing with their corresponding precursor **2aa** and **2ba**, the activities for **4aa** and **4ba** have shown significant increase (94.3% vs 34.1%, 92.6% vs 22.7%). This suggests that the gallic acyl block in these compounds act as a key role to inhibit α-Syn aggregation.

In summary, the amide derivatives of GA, are more efficient inhibitor against α-Syn aggregation than that of GA. Below are a list of active candidates: **1gi** (83.4%), **3g** (84.2%), **3ge** (94.4%), **3gf** (85.5%), **3gh** (91.2%), **4aa** (94.3%) and **4ba** (92.6%). More importantly, their LogP values are in the appropriate range (within 1–3) except **3g** and **4ba**.

2.2.2. IC_{50} study of the representative amide derivatives of GA.

Comparing with GA, the amide derivatives with higher inhibitory activities were selected to perform IC_{50} study (Table 4). The results indicated that the IC_{50} values of **3g**, **3ge**, **3gf**, **3gh**, **4aa** and **4ba** have no distinct differences but all lower than that of GA. Compound **3gh** showed the lowest value (0.98 ± 0.58), and **4ba** displayed slightly higher value than that of GA. More importantly, except for **3g** and **4ba**, they possess appropriate LogP values with a high possibility of crossing the BBB.

2.2.3. The inhibitory kinetics on α-Syn fibrillation and morphology of α-Syn during the conformation transition with and without compounds 3ge, 3gh and 4ba.

Based on the results of IC_{50} study, **3ge** and **3gh** were selected as representative amide derivatives of GA with good inhibitory activities and appropriate LogP values, and **4ba** as another representative with low lipophilicity (LogP 0.74) similar to that of GA (LogP 0.42). The inhibitory kinetic of these compounds to α-Syn fibrillation was investigated under the optimized conditions above. The RFI was measured in 40 μM α-Syn solution incubated with 30 μM of **3ge**, **3gh** and **4ba** respectively (Fig. 2A).

From Fig. 2A, the formation kinetics of α-Syn fibrils without inhibitor (black curve) displayed the entire process including lag phase (formation of β-sheets nucleus), elongation phase (logarithmic increase of β-sheets), and stationary phase (saturation of β-sheets). The addition of compounds **3ge**, **3gh** and **4ba** significantly slowed RFI increase over time, which indicated highly inhibitory effect of these compounds on α-Syn fibril formation.

To confirm the RFI results, the morphology of α-Syn during the conformation transition with and without inhibitor were observed by transmission electron microscope (TEM) (Fig. 2B). Fig. 2B-a showed the image of α-Syn alone after 96 h incubation, which exhibit reticular and bundled fibrils form. Fig. 2B-b showed the image of α-Syn after 96 h

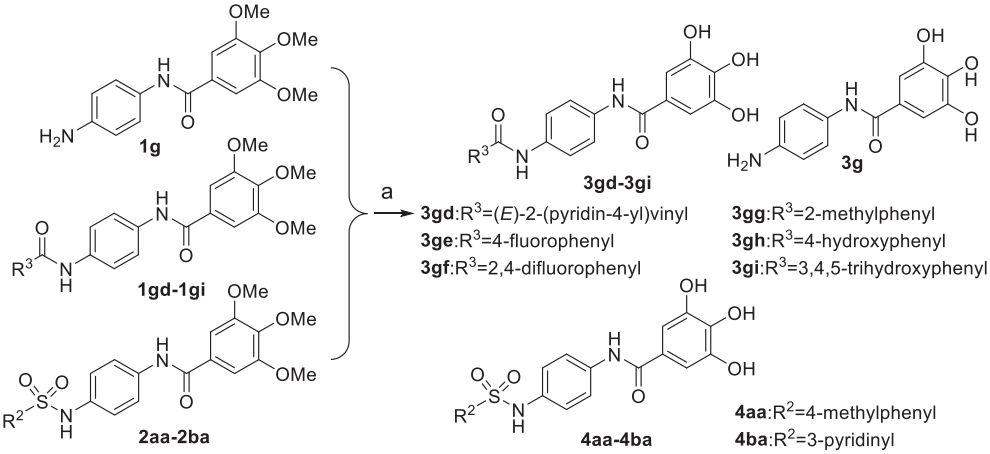

3gd:R^3=(*E*)-2-(pyridin-4-yl)vinyl
3ge:R^3=4-fluorophenyl
3gf:R^3=2,4-difluorophenyl
3gg:R^3=2-methylphenyl
3gh:R^3=4-hydroxyphenyl
3gi:R^3=3,4,5-trihydroxyphenyl
4aa:R^2=4-methylphenyl
4ba:R^2=3-pyridinyl

Scheme 3. Preparation of amide derivatives of GA. Reagents and conditions: a) Dry DCM, BBr_3 (1.0 M in DCM), −78 °C, 20 h, 70–90%.

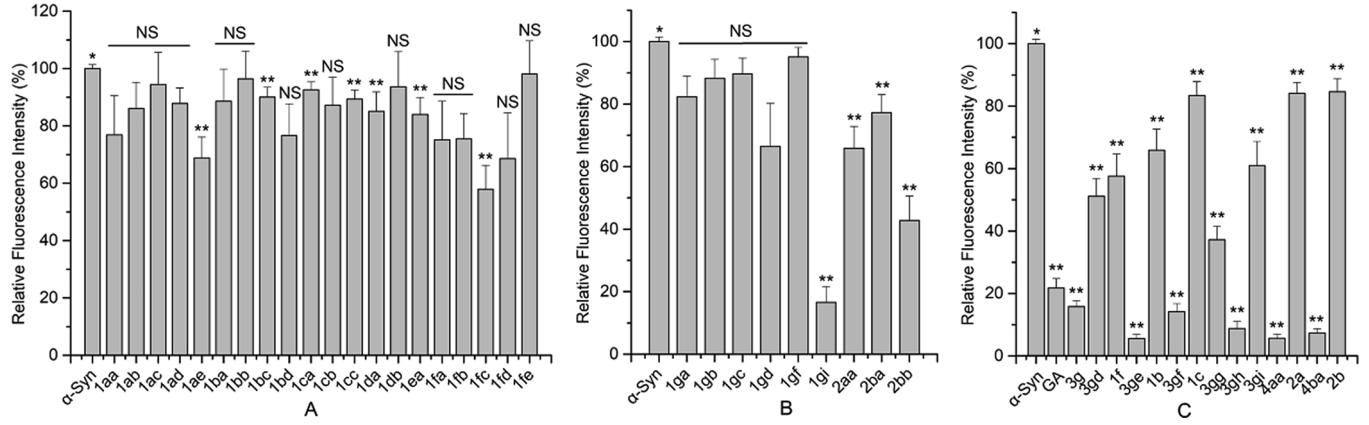

Fig. 1. The ThT RFIs of compounds. A) RFI of **1aa-1fe**. B) RFI of **1ga-2bb**. C) RFI of **1b-1g, 2a-2b**, **GA, 3g, 3gd-3gi** and **4aa-4ba**. Each compound (30 μM) was incubated with 40 μM α-Syn solution in 100 mM PBS (pH = 7.4) for 3 days and then 20 μM ThT was added. Each value is mean of three replicates. NS: no significantly different. (*): $p < 0.05$, (**): $p < 0.01$.

incubation with compound **3ge** at 30 μM. Compared to the severely bundled fibrils in Fig. 2B-a, the fibrils appeared sparsely thinner, revealing an effective inhibition of α-Syn fibrillation by **3ge**. Fig. 2B-c showed the image of α-Syn at the same condition with compound **3gh**. The fibrils appeared more sparsely thinner compared with that in Fig. 2B-b, revealing more effective inhibition by **3gh**. Fig. 2B-d showed the image of α-Syn with compound **4ba**, the fibrils appeared similar with that in Fig.2B-c, also revealing effective inhibition of α-Syn fibrillation by **4ba**.

2.3. Circular dichroism (CD) spectroscopy analysis

To further confirm the influence of potential inhibitor in α-Syn aggregation process, CD spectroscopy was utilized as an efficient method to analyze the variation trend on the secondary structure of the protein by detecting changes in optical activity during protein aggregation.[15]

From Fig. 3, the process of changing on the secondary structure of α-Syn (20 μM) in the presence and absence of compound **3ge**, **3gh** and

Table 1
The SAR study of **1aa-1fe** on α-Syn aggregation.

Cmpd.	R^3	LogP[a]	Ratio[b] (%)	Cmpd.	R^3	LogP[a]	Ratio[b] (%)
	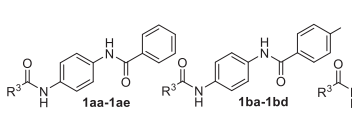						
1aa	Ph-	3.65	23.1	**1cb**		4.28	12.8
1ab		3.8	14.0	**1cc**		4.59	10.6
1ac		3.96	5.6	**1da**		4.28	14.9
1ad		3.96	12.2	**1db**		4.59	6.4
1ae		4.28	31.2	**1ea**		4.91	16.0
1ba		3.96	11.4	**1fa**	Ph-	2.65	24.9
1bb		4.12	3.6	**1fb**		2.81	24.5
1bc		4.12	10.0	**1fc**		2.97	42.1
1bd		4.44	23.4	**1fd**		2.97	31.4
1ca		4.28	7.4	**1fe**		3.28	1.9

[a] Calculated by ChemBioDraw 12.0.
[b] The α-Syn aggregation inhibition ratio of compound at 30 μM.

Table 2
The SAR study of **1ga-1gi** and **2aa-2bb** on α-Syn aggregation.

Cmpd.	R^3	LogP[a]	Ratio[b] (%)	Cmpd.	R^3	R^2	LogP[a]	Ratio[b] (%)
	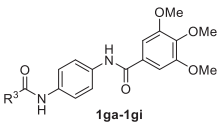 1ga-1gi	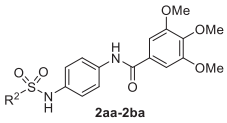 2aa-2ba	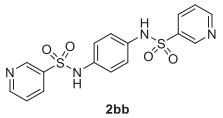 2bb					
1ga	Ph-	3.27	17.7	**1gg**		–	3.75	nd
1gb		3.58	11.8	**1gh**		–	3.14	nd
1gc		3.9	10.4	**1gi**		–	2.89	83.4
1gd		2.27	33.5	**2aa**	–		3.35	34.1
1ge		3.42	nd	**2ba**	–		1.53	22.7
1gf		3.58	4.9	**2bb**	–	–	2.43	57.2

[a] Calculated by ChemBioDraw 12.0.
[b] the α-Syn aggregation inhibition ratio of compound at 30 μM; nd, no detection.

4ba was monitored respectively at initial (0 day) and final time points (3 days) of α-Syn aggregation. The CD spectra were acquired in the range of 190–260 nm.

The CD spectrum of un-incubated α-Syn (initial point) is mainly characterized by a negative signal at 198 nm (−22.7), which is a typical random coil conformation (black line in Fig. 3A). When the incubation time was extended to three days (final point), the signal at 198 nm was attenuated with absolute value of 12 (red line in Fig. 3A), indicating a big decrease in random coil conformation. This result is corresponding to fibril formation of α-Syn (Fig. 2B-a).

On the other hand, α-Syn remained random conformation after the addition of each compound at initial point. Comparing to the black line in Fig. 3A, their negative signal at 198 nm were slightly attenuated (α-Syn + **3ge**: −17.3; α-Syn + **3gh**: −17.9; α-Syn + **4ba**: −19.8), showing that the random coil structure has been reduced, indicating that the added compounds **3ge**, **3gh** and **4ba** may interact respectively with α-Syn, affecting the initial secondary structure of α-Syn (black lines in Fig. 3B–D). After 3 days of corresponding incubation of α-Syn with these three compounds (final point), the negative ellipticity at 198 nm decreased completely (red lines in Fig. 3B-D), but with less extent at the absolute value of 1.3, 1.5 and 7.3 respectively, indicating that such compounds inhibited the conformational transition of α-Syn. These results are also consistent to the inhibitory activities against α-Syn aggregation (from Fig. 2B-b to B-d).

Table 3
The SAR study of **1b-1f**, **3g**, **2a-2b**, **3gd-3gi** and **4aa-4ba** on α-Syn aggregation.

Cmpd.	R^1	R^3	LogP[a]	Ratio[b] (%)	Cmpd.	R^2	R^3	LogP[a]	Ratio[b] (%)
	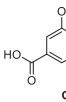 GA	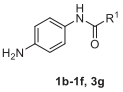 1b-1f, 3g	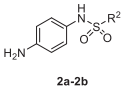 2a-2b	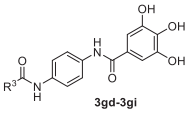 3gd-3gi	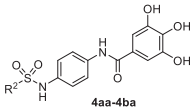 4aa-4ba				
GA	–	–	0.42	78.2	**3gg**	–		2.96	62.8
1b		–	2.19	34.1	**3gh**	–		2.09	91.2
1c		–	2.35	16.6	**3gi**	–		1.31	39.0
1f		–	1.04	42.4	**2a**		–	2.13	15.9
3g		–	0.87	84.2	**2b**		–	0.3	15.4
3gd	–		1.48	48.9	**4aa**		–	2.56	94.3
3ge	–		2.63	94.4	**4ba**		–	0.74	92.6
3gf	–		2.79	85.8					

[a] Calculated by ChemBioDraw 12.0.
[b] The α-Syn aggregation inhibition ratio of compound at 30 μM.

Table 4
IC_{50} study of the representative analogues.

Cmpd.	Structure	LogP[a]	IC_{50} (μM)[b]	Cmpd.	Structure	LogP[a]	IC_{50} (μM)[b]
GA		0.42	4.43 ± 0.68				
3g	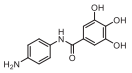	0.87	1.34 ± 0.32	**3gh**	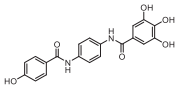	2.09	0.98 ± 0.58
3ge	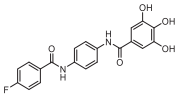	2.63	1.70 ± 0.69	**4aa**	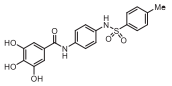	2.56	1.22 ± 0.14
3gf	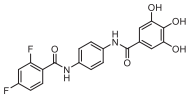	2.79	1.95 ± 0.48	**4ba**	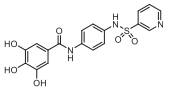	0.74	8.36 ± 1.52

[a] Calculated by ChemBioDraw 12.0.
[b] Each experiment was set up for three days of incubation, and repeated five times at the same concentration.

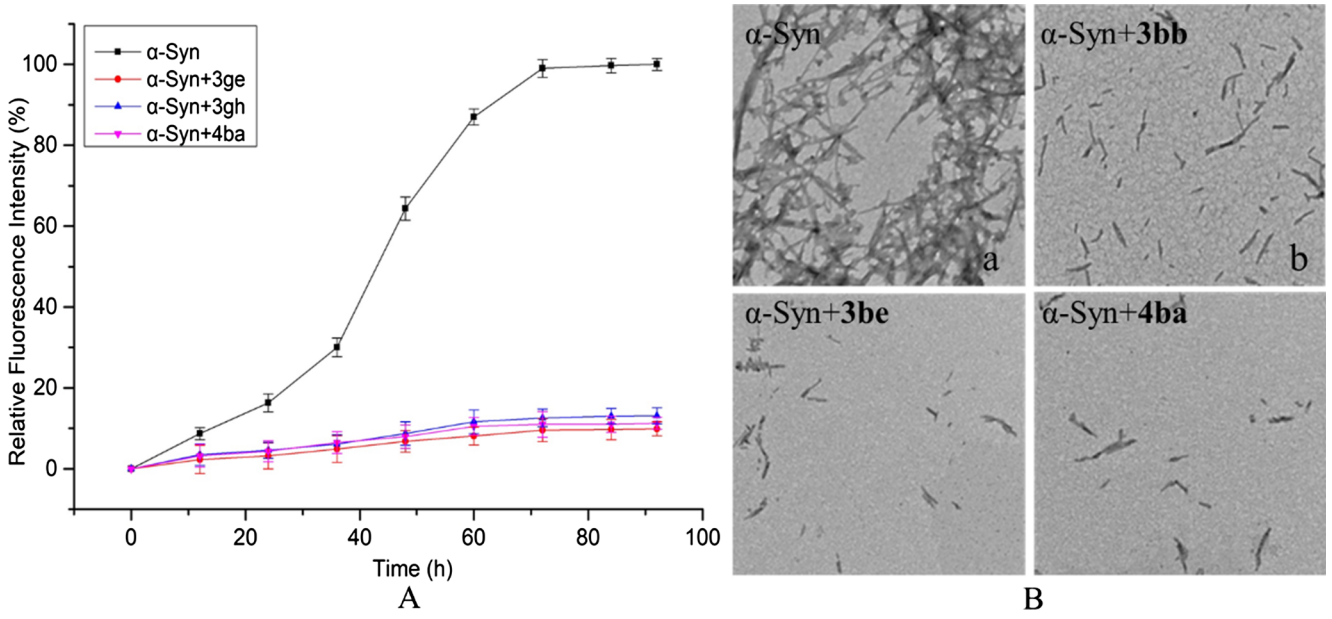

Fig. 2. The inhibition kinetics and morphology on α-Syn fibrillation. A) Inhibition kinetics. α-Syn (40 μM) incubated with and without compound **3ge**, **3gh** and **4ba** at 30 μM respectively, and the experiment was repeated three times. B) Morphology of α-Syn (40 μM) fibrillation after 96 h incubation with and without inhibitors at 30 μM. Scale bar: 500 nm.

Since it has been found anti-oxidative, anti-inflammatory, neuroprotective and inhibitory activity on α-Syn aggregation, GA has received extensive attention, especially on researches about neurodegenerative diseases. Base on the results above, the amide derivatives of GA demonstrated excellent inhibitory activity towards α-Syn aggregation, regardless of protected-hydroxyl or exposed-hydroxyl within GA segment (**1gi** vs **3g**, **3ge**-**3gh**, **4aa**-**4ba**). In general, the latter compounds with exposed-hydroxyl displayed higher inhibitory activity. These molecule possess sheet-like conjugated structure. According to our previous hypothetical mechanism,[4] these compounds tend to parallelly bind the NACore in NAC domain of full-length α-Syn. This binding was considered reversible and it will interfere the formation of nuclei, slowing down the oligomerization process, further inhibiting fibrillation of α-Syn protein. More importantly, most of these compounds possess appropriate LogP value, which may be beneficial for the candidate to cross the BBB as potential inhibitors against α-Syn aggregation.

3. Conclusions

We have designed and synthesized 50 compounds with sheet-like conjugated structural moiety. Among of them, 12 compounds contain methyl-protected GA block, and 9 compounds contain GA block. These conjugated sheet-like molecules, especially the amide derivatives of GA provided robust π-electron delocalized effect and strong hydrogen bonding properties. These analogues have shown anti-aggregation activities *in vitro* towards α-Syn with IC_{50} down to 0.98 μM. The morphology and CD analysis of α-Syn aggregation in the presence and absence of inhibitors have also given the consistent results. This study will be beneficial to PD therapies targeting α-Syn proteostasis in the future.

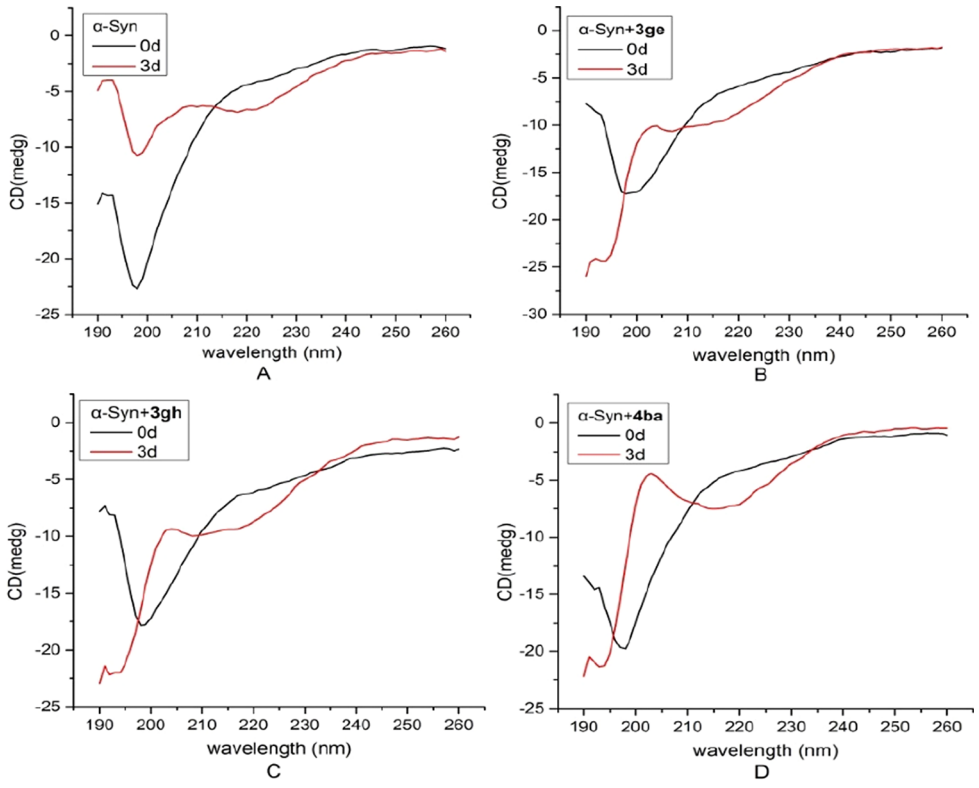

Fig. 3. CD analysis of the secondary structure of α-Syn aggregates formed in the presence and absence of compound **3ge**, **3gh** and **4ba**.

Declaration of Competing Interest

The authors declare that they have no known competing financial interests or personal relationships that could have appeared to influence the work reported in this paper.

Acknowledgments

This work supported by the National Natural Science Foundation of China (31500833 and 81870956), Science and Technology Planning Project of Henan Province of China (192102310141) and the Project for Disciplinary Group of Psychology and Neuroscience in Xinxiang Medical University.

Appendix A. Supplementary data

Supplementary data to this article can be found online at https://doi.org/10.1016/j.bmc.2020.115596.

References

1. (a) Kalia LV, Lang AE. *Lancet.* 2015;386:896–912
   (b) Poewe W, Seppi K, Tanner CM, et al. *Nat Rev Dis Primers.* 2017;3:17013
   (c) Dorsey ER, Elbaz A, Nichols E, et al. *Lancet Neuro.* 2018;17:939–953.
2. (a) Kim C, Lee SJ. *J Neurochem.* 2008;107:303–316
   (b) Maguire-Zeiss KA. *Pharmacol Res.* 2008;58:271–280
   (c) Melki RJ. *J Parkinson's Dis.* 2015;5:217–227.
3. (a) Luk KC, Kehm V, Carroll J, et al. *Science.* 2012;338:949–953
   (b) Knowles TP, Vendruscolo M, Dobson CM. *Nat Rev Mol Cell Biol.* 2014;15:384–396
   (c) Peelaerts W, Bousset L, Van der Perren A, et al. *Nature.* 2015;522:340–344
   (d) Rey NL, Steiner JA, Maroof N, et al. *J Exp Med.* 2016;213:1759–1778.
4. Liu H, Chen L, Zhou F, Zhang YX, et al. *Bioorg Med Chem.* 2019;27:3089–3096.
5. (a) Porat Y, Abramowitz A, Ehud Gazit E. *Chem Biol Drug Des.* 2006;67:27–37
   (b) Ebrahimi A, Schluesener H. *Ageing Res Rev.* 2012;11:329–345.
6. a) Masuda M, Suzuki N, Taniguchi S, et al. *Biochem.* 2006;45:6085–6094
   b) Pandey N, Strider JV, Nolan WC, et al. *Acta Neuropathol.* 2008;115:479–489
   c) Spencer JP, Vauzour D, Rendeiro C. *Arch Biochem Biophys.* 2009;492:1–9
   d) Williams RJ, Spencer JP. *Free Radic Biol Med.* 2012;52:35–45
   e) Rendeiro C, Rhodes JS, Spencer JP. *Neurochem Int.* 2015;89:126–139
   f) Matias I, Buosi AS, Gomes FC. *Neurochem Int.* 2016;95:85–91
   g) Hu Q, Uversky VN, Huang M, et al. *BBA.* 1862;2016:1883–1890
   h) Frandsen JR, Narayanasamy P. *Redox Biol.* 2018;14:465–473
   i) Bakoyiannis I, Daskalopoulou A, Pergialiotis V, Perrea D. *Biomed Pharmacother.* 2019;109:1488–1497
   j) Ahsan N, Mishra S, Jain MK, et al. *Sci Rep.* 2015;5:9862
   k) Suganthy N, Devi KP, Nabavi SF, et al. *Biomed Pharmacother.* 2016;84:892–908
   l) Kose LP, Gulcin I, Goren AC, et al. *Ind Crops Prod.* 2015;74:712–721
   m) Taslimi P, Gulcin I. *J Food Biochem.* 2018;42:e12516
   n) Cakmak KC, Gulcin I. *Toxicol Rep.* 2019;6:1273–1280.
7. (a) Manach C, Scalbert A, Morand C, et al. *Am J Clin Nutr.* 2004;79:727–747
   (b) Cheng B, Gong H, Xiao H, et al. *BBA.* 1830;2013:4860–4871
   (c) Ardah MT, Paleologou KE, Lv G, et al. *Front Aging Neurosci.* 2014;197:1–17.
8. (a) Kim YJ. *Biol Pharm Bull.* 2007;30:1052–1055
   (b) Hansi PD, Stanely MPP. *Chem Biol Interact.* 2009;179:118–124
   c) Reckziegel P, Dias VT, Benvegnu DM, et al. *Toxicol Rep.* 2016;3:351–356.
9. (a) Raina K, Rajamanickam S, Deep G, et al. *Mol Cancer Ther.* 2008;7:1258–1267
   (b) Ohno Y, Fukuda K, Takemura G, et al. *Anticancer Drugs.* 1999;10:845–851.
10. (a) Bastianetto S, Yao ZX, Papadopoulos V, Quirion R. *Eur J Neurosci.* 2006;23:55–64
    (b) LeVine H, Lampe L, Abdelmoti L, Augelli-Szafran CE. *Biochemistry.* 2012;51:307–315
    (c) Liu Y, Pukala TL, Musgrave IF, et al. *Bioorg Med Chem Lett.* 2013;23:6336–6340
    (d) Khan AN, Hassan MN, Khan RH. *J Mol Liq.* 2019;285:27–37.
11. (a) Di Giovanni S, Eleuteri S, Paleologou KE, et al. *J Biol Chem.* 2010;285:14941–14954
    (b) Liu Y, Carver JA, Calabrese AN, Pukala TL. *BBA.* 1844;2014:1481–1485.
12. (a) Lardeau A, Poquet L. *J Pharm Biomed Anal.* 2013;76:134–138
    (b) Dichiara M, Amata B, Turnaturi R, et al. *ACS Chem Neurosci.* 2020;11:34–44.
13. Bhatt V, Samant SD, Pednekar S. *Lett in Org Chem.* 2017;14:764–768.
14. Perin N, Roskaric P, Sovic I, et al. *Chem Res Toxicol.* 2018;31:974–984.
15. Jha NN, Kumar R, Panigrahi R, et al. *ACS Chem Neurosci.* 2017;8:2722–2733.